THE ASTRONOMICAL JOURNAL VOLUME 112, NUMBER 3 SEPTEMBER 1996

NEUTRAL HYDROGEN AROUND EARLY-TYPE GALAXIES

KIMBERLY DUPRIE[1] AND STEPHEN E. SCHNEIDER

Five College Astronomy Department and Department of Physics and Astronomy, University of Massachusetts, 536 Lederle Tower, Amherst, Massachusetts 01003

Electronic mail: schneide@phast.umass.edu

Received 1996 April 8; revised 1996 June 4

ABSTRACT

When early-type (E,S0) galaxies have neutral hydrogen gas associated with them, it is often located over a very extended region. This suggests several possible origins for the gas, either intrinsic to the galaxy or from an external source. We present 21 cm H I maps around early-type galaxies to study the distribution of gas in the galaxies' vicinity and address these possibilities. We examine two sets of objects: (1) early-type galaxies with conflicting H I measurements that might indicate unusual gas distributions, and (2) galaxy groups that are dominated by early-type galaxies. We have identified several galaxies with extended H I disks, and a number of H I companions that may be interacting with the early-type galaxies and may be confusing H I observations. Many of the companions can be optically associated with uncataloged dwarf galaxies, but a few are quite peculiar or have no clear optical association. We discuss the implications of these results for the origin of H I in early-type galaxies. © *1996 American Astronomical Society.*

1. INTRODUCTION

The neutral hydrogen in lenticular and elliptical galaxies presents a puzzle. Its properties do not extrapolate from the sequence seen progressing from Sc to Sa galaxies; instead most Es and S0's contain virtually no H I, but occasionally they have a large amount of gas, which is often distributed over an extended region outside of the optical disk of the galaxy. If the gas in spiral and irregular galaxies accounts for continuing star formation and its dissipative effects help shape the galaxies' structure, then the presence of large amounts of gas in some early-type galaxies would require a different explanation. The distribution of H I in and around early-type galaxies may also provide clues about the forces that generate these morphological differences. In this paper we describe a series of observations undertaken to better understand the context of early-type galaxies and their H I.

Previous studies of H I in early-type galaxies have focused mostly on basic detection statistics, but it is clear that the distribution of gas is sometimes unusual and that its presence may be related to the galaxies' environment. In addition, the long integrations employed in these detection surveys can lead to deceptive results: if the gas is not confined to the inner part of the galaxy, deep single-dish observations may detect H I from confusing sources at the edge of the beam or in its sidelobes. Even if the gas is associated with the early-type galaxy, single-dish observations may not give an accurate estimate of the amount present if the gas is not centrally located in the galaxy. This is in fact what van Driel & van Woerden (1991) found in radio synthesis observations—that the hydrogen in lenticulars is frequently distributed in an extended disk or ring, residing primarily outside of the bright optical disk of the galaxy.

Several H I surveys have probed the regions surrounding galaxies. For example, nearby groups of galaxies were studied by Lo & Sargent (1979) and by Haynes (1981), uncovering an assortment of apparently tidal structures mostly around later-type galaxies. One aspect of the present project is to extend this work to very early galaxy types, where relatively little gas is expected to be contributed by the large galaxies themselves. In this way, there is less probability of the extended/external gas having arisen from the galaxy itself during a recent tidal encounter or stripping event. The survey of early type galaxies by van Driel & van Woerden (1991) demonstrated that the H I in these systems is unusual; with the Arecibo telescope,[2] we can extend the coverage to larger areas with greater sensitivity.

Another motivation for this project was the intergalactic gas detected in the M96 group (Schneider 1989). This H I feature extends over more than 1° in the form of a ring surrounding the S0 and E galaxies at the center of the group. In some respects this ring might be regarded as an extreme example of the extended disk and ring features found by van Driel & van Woerden. Mapping the large regions surrounding early-type galaxies would help determine whether gas is common in structures larger than the extended disks found in synthesis-array observations, and the contextual relationship of the gas might point toward its origin.

Eder *et al.* (1991) find that early-type galaxies in low density environments tend to have higher total H I masses relative to their optical area. It seems likely that the hot intracluster medium in clusters and dense groups ionizes or strips away any outer H I. Therefore we restrict our examination to

[1]Current address: Harvard-Smithsonian Center for Astrophysics, 60 Garden Street, MS 81, Cambridge, MA 02138.

[2]The Arecibo Observatory is part of the National Astronomy and Ionosphere Center which is operated by Cornell University under cooperative agreement with the National Science Foundation.

early-type galaxies in the field and in low-density groups. We have identified a number of galaxies that have discrepant levels of H I recorded in the literature, anticipating that an extended gas distribution might have given rise to contradictory flux measurements by radiotelescopes with different beam sizes. We also select several nearby groups of galaxies that, like the M96 group, are dominated by early-type galaxies, to see if other large H I structures are present.

We describe the technical details of these observations in Sec. 2. The selection procedures and observational results are described in Secs. 3 and 4 for the two sets of galaxies that we examined. Finally, we discuss the general results of the survey and their possible interpretation in Sec. 5.

2. OBSERVATIONAL TECHNIQUE

Initial observations were carried out at the Arecibo Observatory in 1986 with follow-up observations in 1993 and 1994. Both the dual-circular polarization and linear polarization ("flat") 21 cm feeds were available, but most of the observations were carried out with the circular feed. The main difficulty with the circular feed is that its first sidelobe has ~10% of its forward gain, which is a potential source of confusion; nevertheless, it was deemed best for the present study for most of the observations because of its much higher sensitivity and stability (see Schneider *et al.* 1986). Only one galaxy (NGC 5701) proved to have such extended H I in such a narrow velocity range that follow-up flat feed observations were necessary.

The observations were carried out in a hexagonal or "honeycomb" pattern, which offers more efficient coverage of the sky than the standard rectangular pattern (Schneider 1989). In most instances a beam spacing of 3.′8 was used. The dual-circular feed has a beam width (FWHM) of ~3.′3 and a first sidelobe at 5.′4 from the beam center. There is a null at ~3.′7, which is close to the beam spacing in our pattern so signals detected at points adjacent to a detected source are relatively unlikely to be caused by spillover from the neighboring position.

The 3.′8 beam spacing also provides complete coverage of the area observed (Schneider 1989). At spacings at least this small, the "summed beam" over all the points in the observing grid has nearly uniform sensitivity. This allows us to add up the individual spectra to find the total flux from an extended object, with a correction factor of 1.05–1.25 in our case (depending on the number and distribution of beams summed), to account for the effective forward gain of the summed beam. In a few cases, a beam spacing of 7.′6 was used to map out a larger area, or a beam spacing of 1.′9 (full-sampling) was used to achieve more detail. In one instance a beam spacing of 15.′2 was used in order to rapidly survey a very large region to determine if any very extended H I was present.

In the regions mapped with complete coverage, we should detect any extended source with a column density greater than 10^{19} cm^{-2} (for a linewidth of 50 km s^{-1} and a typical rms of 2 mJy). For a source within the beam we are sensitive to a mass $\gtrsim 3\times10^7\ \mathcal{M}_\odot \times (d/20\ \mathrm{Mpc})^2$. In the sparsely mapped areas we could have missed a badly placed object smaller than ~30 kpc in the two groups mapped at 7.′6 spacing, and ~80 kpc in the one group mapped at 15.′2 spacing. In these same groups, however, the circular feed's sidelobes would have picked up sources with about 10% of the sensitivity of the main beam over most of the unmapped portions.

The flat feed was used for observations of NGC 5701, which our initial circular-feed observations showed to have a very extended H I distribution. The flat feed has a beam width of ~4.′0 with a <2% first sidelobe at ~6.′ Its properties are described in detail by Corbelli *et al.* (1989). For the observations reported here, the flat feed was used with a grid spacing of 3.′8, or 12.5 arcmin^2 per beam. Given the extent of the H I observed, and summing up the total effective beam from a detailed profile of the flat-feed beam, the effective forward gain is ~1.3 times the single beam value when all the beams are added in these observations.

The Arecibo telescope has an altitude-azimuth configuration in which the spherical dish remains fixed and the feeds point to different zenith angles. As a result, different zenith angles receive different levels of ground radiation and interference, with the most ground radiation received at large zenith angles. For this reason, the maps (and sometimes individual spectra near the beginning or end of a map) achieve different sensitivities for the same integration time. The observations were usually made near the smallest zenith angles possible for the declination of the source, and integration times ranging from 60 to 180 s per point were chosen to partially compensate for the zenith angle effects.

The data were analyzed using Arecibo's data reduction package ANALYZ. A single observation point was used as the *on* scan, and the *off* scan consisted of an average of all of the observation points in that run. Because the zenith angle was changing between *on* and *off* scans, fairly large changes in the total power entering the telescope front end were common, leading to non-linearities in the baselines. Therefore, baselines were fit with polynomials to regions where no signal was evident. After Hanning smoothing, the spectral resolution was 16 km/s and the channel-to-channel rms around the baseline fit was typically ~2 mJy. In addition, the flat-feed data were corrected for standing wave problems by subtracting components in the Fourier transform of the spectra.

Most detections would stand out quite clearly as a moderately wide "bump," easily distinguishable from sharp interference spikes and background noise, but much narrower than baseline irregularities. Most of the suspected signals were reobserved with longer integration times to provide confirmation, although this was not possible in a few instances. In the unconfirmed cases, which we call attention to in the detailed notes later, we have checked to make sure that interference was not otherwise present at the same frequency and that the signal was consistent in the left and right circular polarizations.

Total fluxes were determined from the integrated signal under the line profiles, and mean (heliocentric) velocities and widths were determined at 50% of the peak flux densities in the two "horns" of the profile. In the widely-spaced observations of groups, our fluxes, velocities, and linewidths are subject to fairly large uncertainties because the telescope beam was not necessarily centered on the galaxy's coordi-

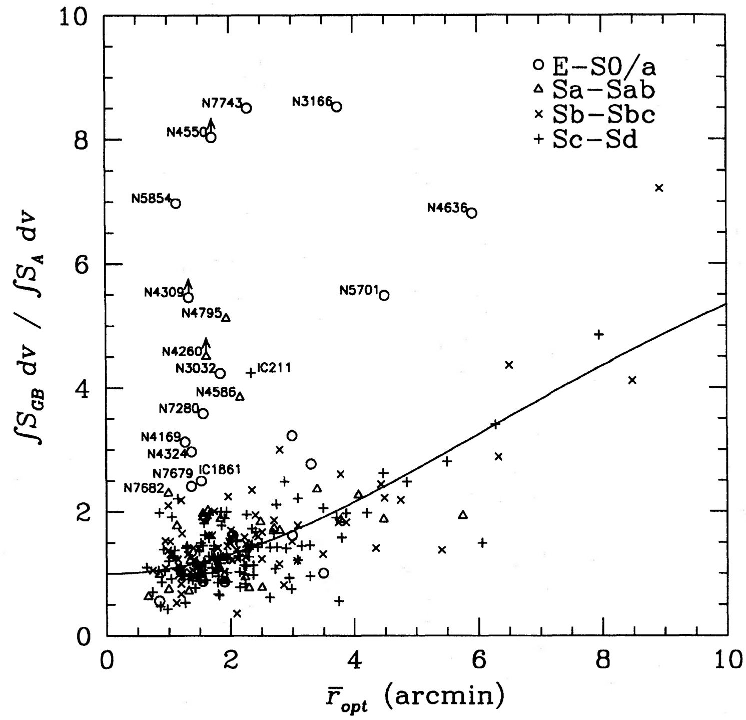

FIG. 1. Ratio of Green Bank and Arecibo integrated fluxes compared to their optical sizes. Different ranges of types are shown by different symbols, and the line shows the expected relationship if the H I and optical sizes are the same. Galaxies with discrepancies greater than a factor of 2 are labeled according to their NGC and IC numbers.

nates. In the more tightly-spaced observations, the galaxies were usually close to an individual beam or we were able to sum up several neighboring beams to obtain a complete H I profile, so these data are more reliable.

3. GALAXIES WITH DISCREPANT FLUX MEASUREMENTS

3.1 Selection Procedure

In an attempt to identify early-type galaxies with unusually large amounts of H I, we compared flux measurements from large-beam telescopes, like Green Bank, with those from Arecibo. One would expect that for galaxies smaller than the Arecibo beam, the flux measurements should be nearly equal; but for galaxies with H I more widely distributed than the Arecibo beam, the Green Bank flux should be larger. We can use this principle to test the size of the H I distribution relative to the cataloged optical size.

Assuming the two telescope beams can be approximated by Gaussians with sizes (FWHM) θ_1, θ_2, and the galaxy's H I distribution can likewise be treated as a two-dimensional Gaussian with major and minor axis sizes of a and b, the expected flux ratio is

$$\frac{\int S_1 dv}{\int S_2 dv}=\left(\frac{\theta_1}{\theta_2}\right)^2\left[\frac{(\theta_2^2+a^2)(\theta_2^2+b^2)}{(\theta_1^2+a^2)(\theta_1^2+b^2)}\right]^{1/2}. \qquad (1)$$

For the beam sizes of Arecibo ($\sim$3$'$.3) and Green Bank ($\sim$10$'$.5), the ratio ranges from 1 for small galaxies, and approaches 9 for galaxies much larger than the Green Bank beam. The actual data for an assortment of UGC galaxies observed at both Arecibo and Green Bank are plotted in Fig. 1 along with the curve for Eq. (1) where $\bar{r}_{opt}$ equals the mean ($\sqrt{ab}$) optical diameter from the UGC. (Where Green Bank data were unavailable, we have used data from the Efflesburg 100 m telescope, which has a similar beam size.) The galaxies shown in the figure are those recorded in the Huchtmeier & Richter (1989) bibliographic catalog of H I observations, using only those references that give central beam measurements.

Figure 1 shows that most galaxies follow the expected ratio of fluxes, albeit with a fairly large scatter that is probably caused by noise and calibration uncertainties in the radio flux measurements. Several galaxies deviate by more than a factor of 2 from the predicted flux ratio, and have been labeled in the figure. The most extreme galaxies approach the upper limit for flux ratios supposing the disks were much more extended than the 10$'$.5 Green Bank beam.

The objects that most commonly have deviant H I ratios, and the most deviant objects, are early-type galaxies. This indicates that the H I detected in early-type galaxies is more likely to be located, on average, farther from their centers. Some possible explanations for this behavior are that the early-type galaxies: (1) are often surrounded by extended disks of H I; or (2) have nearby gas in faint dwarfs or intergalactic clouds. Unfortunately, because of the long integration times necessary to detect the weak H I emission in early type galaxies, it is also true that they: (3) are more likely to

TABLE 1. (a). Mapped regions around discrepant-flux galaxies.

Region # (1)	Name (2)	R.A. Range (3)	Dec. Range (4)	N (5)	Beam Spacing (arcmin) (6)	t_{int} (min) (7)	rms (mJy) (8)
1	IC 1861	$02^h49\overset{m}{.}1-02^h51\overset{m}{.}0$	25°09′–25°27′	48	3.8	2.0	2.5
2	NGC 3032	09 48.1–09 50.6	29 14–29 40	70	3.8	2.0	1.7
		09 49.4–09 50.4	29 27–29 38	60	1.9	2.0	1.8
3	NGC 3788/6	11 36.2–11 37.7	32 04–32 23	30	3.8	1.0	2.0
4	NGC 3801	11 36.9–11 38.2	17 55–18 07	18	3.8	3.0	1.2
5	NGC 4260	12 16.1–12 17.3	06 10–06 30	30	3.8	3.0	1.7
6	NGC 4324	12 19.6–12 21.3	05 21–05 40	32	3.8	2.0	2.1
7	NGC 4550/1	12 32.0–12 34.2	12 34–12 50	80	3.8	2.0	1.3
8	NGC 4636	12 39.4–12 41.1	02 46–03 13	55	3.8	2.0	3.6
9	NGC 4795	12 51.8–12 53.5	08 04–08 30	56	3.8	1.0	1.7
10	NGC 5701	14 35.5–14 37.8	05 15–05 46	90	3.8	1.5	2.3
		14 35.1–14 37.8	05 15–05 50	100	3.8	2.0	4.0
		14 33.7–14 38.9	05 07–05 57	168	7.6	1.0	3.3
11	NGC 5854	15 04.5–15 05.8	02 35–02 53	30	3.8	2.0	1.8
12	UGC 10528	16 41.9–16 43.8	22 28–22 48	40	3.8	2.0	1.5
13	NGC 7280	22 23.2–22 25.0	15 45–16 05	63	3.8	2.0	1.5
14	NGC 7679	23 25.4–23 27.3	03 01–03 25	24	3.8	1.0	2.5
15	NGC 7743	23 40.8–23 43.0	09 30–09 58	57	3.8	1.5	1.3

suffer from confusion with distant galaxies; or (4) have larger uncertainties associated with "baseline instabilities" caused by solar interference, unstable receivers, etc.

To determine the source of these discrepancies, we observed most of the early-type galaxies identified in Fig. 1, along with a selection of objects for which we had questions based on differences in spectra taken at Arecibo. There are a few objects meeting our criteria that we did not observe here. Most of these were studied elsewhere or were excluded based on our selection criteria: NGC 3166 is part of the group Vennik 30 studied in the next section. NGC 4169 was excluded because it is part of a compact group (see Hickson *et al.* 1992). NGC 4586 has been mapped along its major axis previously by Helou *et al.* (1984), and the flux difference appears to be mainly due to uncertainties in the earlier fluxes.

Two objects probably should have been included in the survey, and would be interesting candidates for additional study: NGC 4309 has an upper limit at Arecibo much lower than a detection reported at Efflesburg and was omitted for lack of observing time. And we realized too late that the only discrepant Sc galaxy, IC 211, is only 4′.5 away from an unstudied S0 galaxy NGC 851, so the discrepancy may actually be related to the early-type galaxy.

In Table 1(a) the galaxies with discrepant fluxes chosen for this study are listed. The map sequence number is listed in column (1) and the name of the galaxy studied, or the brightest galaxy in the group is listed in column (2). The right ascension and declination (1950) ranges are listed in columns (3) and (4). The number of points in the map is listed in column (5), and column (6) gives the spacing between points on the map. Column (7) gives the integration time per point, and column (8) gives the average rms of the spectra in the map.

3.2 Results of the Observations

A summary of the detections and upper limits is given in Table 1(b). Column (1) lists the map number, while column (2) lists the object's common name. Some detected objects were uncataloged; in these cases we assign a name based on the truncated 1950 coordinates. The coordinates of the detection are given in columns (3) and (4). If the object was detected at more than one point, the coordinates of the strongest detection are reported. The morphological classification of each galaxy as given in the *Third Reference Catalog* (de Vaucouleurs *et al.* 1991, hereafter referred to as RC3) is listed in column (5). The detected flux is listed in column (6). Column (7) lists the heliocentric velocity while column (8) contains the velocity width at 50% of the peak. The assumed distance to the object or group in column (9) is based on the Galactocentric velocity using a Hubble constant of 75

TABLE 1. (b). H I measurements around discrepant-flux galaxies.

Map # (1)	Object (2)	R.A. (3)	Dec. (4)	Type (5)	$\int S\,dv$ (Jy km s^{-1}) (6)	V_{hel} (km s^{-1}) (7)	ΔV_{50} (km s^{-1}) (8)	D (Mpc) (9)	$M_{\rm H\,I}$ ($10^9 M_\odot$) (10)	$\theta_{\rm H\,I}$ (arcmin) (11)	$\theta_{\rm opt}$ (arcmin) (12)	B_T^0 (13)
1	IC 1861	$02^h50^m11\overset{s}{.}9$	25°17′00″	SA0	2.2	6687	417	91	4.2		1.62	13.61
2	NGC 3032	09 49 14.1	29 28 20	SAB(r)0	0.9	1550	161	19	0.076		1.95	12.84
2	0949+2935	09 49 52.0	29 35 00		1.3	1456	106	19	0.11			
2	0950+2931	09 50 03.0	29 31 40		0.9	1650	56	19	0.076			
3	NGC 3788	11 37 06.2	32 12 35	SAB(rs)ab	10.3	2674	445	36	3.1	3.2	2.14	12.80
3	NGC 3786	11 37 04.4	32 11 08	SAB(rs)a(pec)		— not detected —					2.19	12.97
4	NGC 3801	11 37 41.3	18 00 24	S0?	~2.2	3451	574	45	2.1		3.24	12.79
4	NGC 3790	11 37 11.8	17 59 26	S0/a	1.5	3385	372	45	0.7		1.0	14.44
4	MCG+03-30-035	11 37 28.1	17 58 18		2.3	3872	251	45	1.1		0.8	16
4	NGC 3806	11 38 10.8	18 04 18	SABb	5.7	3495	152	45	2.7		1.4	14.05
5	VCC 329	12 16 35.5	06 15 05	I?	0.23	1603	77	17	0.016		0.3	
5	NGC 4260	12 16 48.8	06 22 40	SB(s)a		— not detected —					2.7	12.31
5	VCC 340	12 16 48.7	06 13 11		1.9	1514	75	17	0.13		0.6	15.34
5	VCC 379	12 17 15.1	06 16 59		0.39	1462	31	17	0.026			
5	VCC 405	12 17 41.5	06 16 59	dE0	1.1	2097	282	17	0.075			
5	1218+0615	12 18 21.1	06 15 05		0.42	1758	99	17	0.029			
6	NGC 4324	12 20 32.5	05 27 49	SA(r)0+	9.3	1637	301	17	0.63	7.6	2.5	12.52
7	NGC 4550	12 32 59.3	12 29 48	SB0		— not detected —					2.8	12.36
7	NGC 4551	12 33 06.6	12 32 27	E		— not detected —					1.8	12.76
8	NGC 4636	12 40 16.6	02 57 43	E0+		— not detected —					5.8	10.43
9	NGC 4795	12 52 31.6	08 20 15	SB(r)aP	1.9	2810	282	36	0.57	7.6	1.9	13.01
9	UGC 8042/5	12 52 44.8	08 10 46	S?	1.5	2732	261	36	0.45		1.3	14.47
10	NGC 5701 "cloud"	14 35 48.6	05 38 40		6.5	1503	39	20	0.61	5.		
10	NGC 5701	14 36 41.5	05 34 50	(R)SB(rs)0/a	51.9	1505	121	20	4.9	20.	4.4	11.65
11	NGC 5854	15 05 16.7	02 45 37	SB(s)0+		— not detected —					2.3	12.69
12	UGC 10528	16 42 42.2	22 36 41	SA0+	6.9	4261	488	59	5.6		2.2	12.89
13	NGC 7280	22 24 01.5	15 53 40	SAB(r)0+	1.02	1817	186	28	0.18		2.1	12.84
13	UGCA 429	22 24 15.1	15 55 34	Im	5.2	1900	113	28	0.94		1.1	14.89
14	NGC 7679	23 26 12.7	03 14 11	SB0p:	5.7	5138	269	69	6.4		1.4	12.89
14	NGC 7682	23 26 25.9	03 16 05	SB(r)ab	4.2	5135	184	69	4.7		1.3	13.67
14	UGC 12628	23 26 47.8	03 06 37	SB(rs)c:	4.2	4678	170	69	4.7		1.6	14.49
15	2341+0947	23 41 35.2	09 47 01		0.47	1610	50	24	0.064			
15	2341+0948	23 41 48.5	09 48 55		3.3	1509	122	24	0.45	3.2		
15	NGC 7743	23 41 48.6	09 39 25	(R)SB(s)0+		— not detected —					3.0	12.16

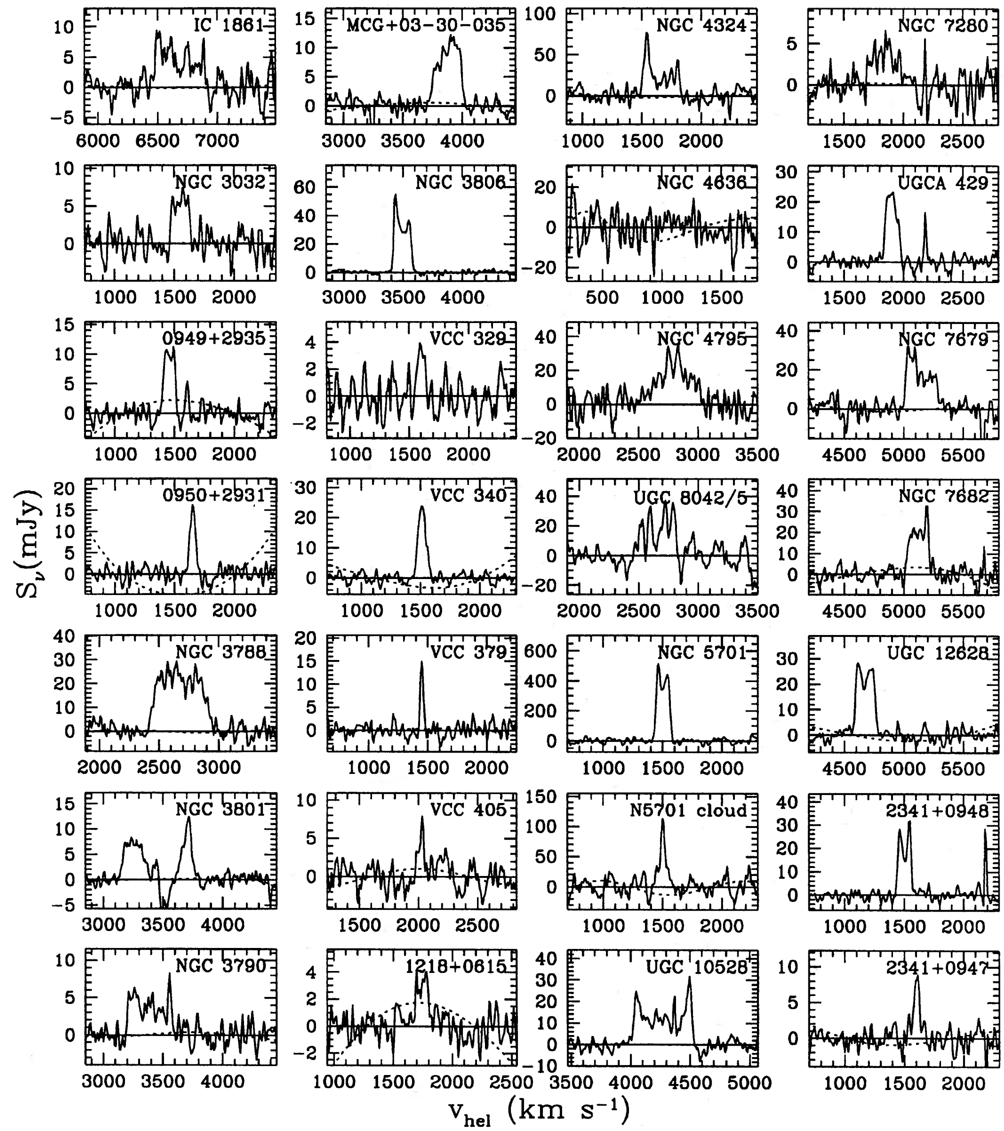

FIG. 2. H I spectra of the objects detected in the mapping of galaxies with discrepant H I measurements. The galaxies are in order of R.A., and for close members of the same group, the same 1500 km s^{-1} range in redshift is shown for all. The dotted line shows the effect of the baselining procedure on a straight line to give an indication of how the observations might have been affected.

km s^{-1} Mpc^{-1}. Galaxies in the general vicinity of the Virgo Cluster are assigned a distance of 17 Mpc. The mass of neutral hydrogen as determined by the equation

$$\mathcal{M}_{\rm H\,I}=2.35\times 10^5 d^2 \int S_{\rm H\,I} dv$$

is given in column (10). The angular extent over which the galaxy was detected, if it was seen in more than one beam, is listed in column (11). Columns (12) and (13) contain the optical size and corrected magnitude from the RC3. The corresponding spectrum for each detection is shown in Fig. 2.

We discuss the individual maps in more detail below where we also discuss previous observations. When data from Green Bank is quoted, it is from the 300 foot telescope unless otherwise noted.

1: IC 1861 (S0). Fluxes as low as 1.8 Jy km s^{-1} were reported from Arecibo and as high as 5.4 Jy km s^{-1} from Green Bank. This is the highest redshift galaxy examined, and therefore our sensitivity to low level emission is relatively poor. We detect no sign of extended emission, and based on examination of the Green Bank spectra, we suspect those measurements are probably overestimated.

2: NGC 3032 (S0). Fluxes of 1.0–1.3 Jy km s^{-1} were reported at Arecibo and 5.3 Jy km s^{-1} at Green Bank. Our observations of NGC 3032 match the Arecibo measurements, and no additional emission is found in any of the

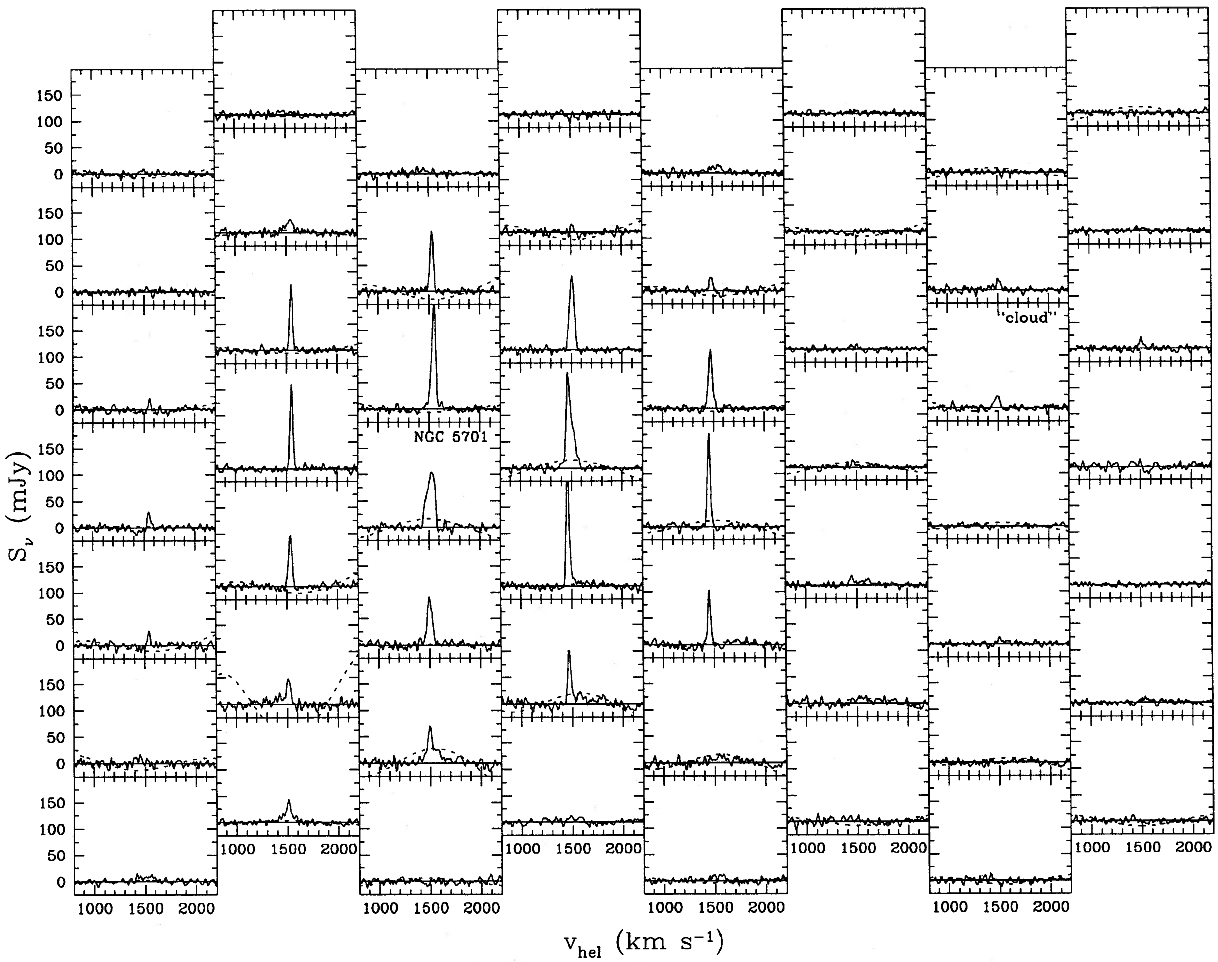

FIG. 3. Flat-feed map of NGC 5701 and H I "cloud" to its northwest. Points on the hexagonal grid are separated by 3.'8 from their neighbors. NGC 5701 has an optical extent of only ~4.'5, and is centered about 1.'5 northwest of the spectrum labeled with its name.

points immediately surrounding the galaxy. However, about 10′ to the northeast, there is a complex H I distribution that we mapped out with a finer grid spacing. There appear to be two distinct objects: 0950+2931 is a single-horned H I profile probably associated with a small, relatively high surface brightness dwarf visible on the Palomar plate and listed in the Kiso Ultraviolet Galaxy Catalog (Takase & Miyauchi-Isobe 1986) as KUG 0950+295. The other object, 0949 +2935, is ~4′ northwest of the other. It has a double-horned profile, which is normally indicative of a rotating disk galaxy, but only a few extremely faint features are visible on the Palomar plate, which have no clear organization into a classifiable galaxy. Curiously, a faint *IRAS* source, F09499 +2935, is listed only ~1′ from the coordinates of this object. A more detailed study of this system is in preparation.

3: NGC 3788/6 (Sab/Sa). This close pair (separation 1.'5) has had a wide range of inconsistent fluxes reported. Arecibo fluxes of 9.4–12.9 Jy km s^{-1} were reported for NGC 3788, and 4.9–12.1 Jy km s^{-1} for NGC 3786. A Green bank flux of 15.4 Jy km s^{-1} was listed for NGC 3786. We detect H I centered on NGC 3788 which appears extended over ~3.'2, but NGC 3786 was not detected. The limited snap-shot Westerbork map of Oosterloo (1988) appears to confirm this interpretation, although he regarded his results as inconclusive.

4: NGC 3801 (S0?). This map covers a complicated region containing a number of galaxies probably forming a group, although it is not identified as such in the standard catalogs. A large number of observations have been made of NGC 3801 and the galaxies surrounding it with various disagreements about fluxes and velocities. In addition, previous spectra showed a possible large H I absorption feature in NGC 3801, which we suspected might have instead been produced by a complex of separate features. However, our spectrum confirms the original interpretation as an absorption feature. We mapped a relatively small region, but detected emission in several locations. We detected H I from two galaxies neighboring NGC 3801 that had not previously been detected, including NGC 3790 (SO/a) and an *IRAS* source MCG +03−30−035. The *IRAS* source is only 3.'6 distant, but its systemic velocity differs by more than 400 km s^{-1}. We extrapolate across the absorption feature in NGC 3801 to estimate the total emission so this value is uncertain.

We also detected NGC 3806 but not NGC 3802, another close companion.

5: NGC 4260 (Sa). An upper limit of 0.7 Jy km s^{-1} was reported at Arecibo while a detection of 3 Jy km s^{-1} was reported at Effelsberg. The nearby galaxy UGC 7349 also had an Arecibo detection at 5500 km s^{-1} and one at Parkes at 980 km s^{-1}. We detect nothing at the positions of NGC 4260 or UGC 7349 (up to a velocity of 3600 km s^{-1}). In the general vicinity, four objects listed in the Virgo Cluster Catalog (Binggeli *et al.* 1985, hereafter referred to as VCC) have possible detections. A fifth possible source (1218+0615) was found near a position where a very faint, uncataloged (possibly background) galaxy appears on the Palomar plate. VCC 329 and 340 have previous detections consistent with our measurements after accounting for the offsets in our positions from the galaxy centers. It appears possible that the detection at Effelsberg was caused by confusion with VCC 340. VCC 379 and 405 are listed as dwarf ellipticals, which would make H I detections surprising, but we caution that none of these positions has been reobserved.

6: NGC 4324 (S0). Fluxes at Arecibo as low as 3.4 Jy km s^{-1} were reported, while the flux at Effelsberg was given as 10.1 Jy km s^{-1}. We detect H I centered on NGC 4324 extending over 7.'6 in the map. Hoffman *et al.* (1989) made a major axis map of this galaxy and also conclude that it has an extended disk, which appears to be similar in extent to a faint outer optical ring noted in the VCC.

7: NGC 4550/1 (S0/E). Arecibo reported less than 1 Jy km s^{-1} while Green Bank reported 9.03 Jy km s^{-1} for NGC 4550. Arecibo reported 0.13 Jy km s^{-1} for NGC 4551. We detect nothing for either galaxy down to a flux density of $\lesssim$1.5 mJy.

8: NGC 4636 (E). Conflicting values have been reported from Arecibo of <1.16 Jy km s^{-1} or a possible detection of 2.37 Jy km s^{-1}, and a Green Bank and Nançay detections of ~16 Jy km s^{-1} have also been recorded. We do not detect any channels $\gtrsim$8 mJy over the velocity range of these reported detections in the sum of the six beams covering the optical extent of the galaxy (shown in Fig. 2). We estimate an upper limit to the integrated flux of $\lesssim$2 Jy km s^{-1} over the ~600 km s^{-1} width claimed at Green Bank, although baseline uncertainties (in both our spectrum and that at Green Bank) make this somewhat uncertain.

9: NGC 4795 (Sa). Fluxes of 0.3–1.2 Jy km s^{-1} were reported at Arecibo while at Effelsberg 6.3 Jy km s^{-1} was reported. We detect weak signals at the position of NGC 4795 and at surrounding points. The signals appear to grow stronger in the direction of the companions UGC 8042/5, which are also detected (although we cannot separately distinguish them with these observations). It is possible that there is a tidal stream between NGC 4795 and its irregular companions.

10: NGC 5701 (S0/a). Arecibo reported 9.9 Jy km s^{-1} while Green Bank reported between 40 and 50 Jy km s^{-1} and Nançay reported 58 Jy km s^{-1}. We originally mapped this galaxy with the circular feed and found that the H I extended over 20.' Because the H I is so extended, we re-observed this galaxy with the flat feed to reduce sidelobe contamination, and data from the flat-feed spectra are reported in Table 1(b) and shown in Fig. 3. The H I around NGC 5701 appears to be in a regular disk, following a smooth rotation curve with no obvious sign of interaction or warping. There is, however, a separate H I "cloud" ~15′ to the northwest that has no optical counterpart. NGC 5701 appears to be quite isolated on the sky optically, and we searched over ~1 deg^2 with a coarse grid and found no evidence for other H I sources in the vicinity.

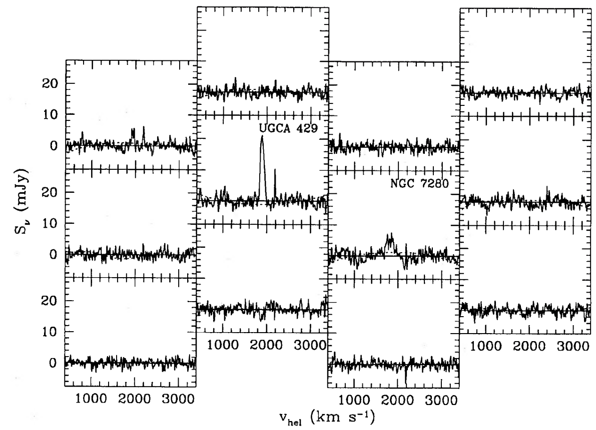

FIG. 4. Portion of H I map around NGC 7280. Points on the hexagonal grid are separated by 3.'8 from their neighbors.

11: NGC 5854 (S0). A number of upper limits have been reported for this galaxy along with a flux of 0.43 Jy km s^{-1} reported at Arecibo and 3 Jy km s^{-1} found at Effelsberg. We detect no extended emission in neighboring points that might account for the discrepancy. Unfortunately, uncertain baseline subtraction at the position of the galaxy itself does not allow us to confirm either flux measurement.

12: UGC 10528 (S0). Fluxes of 4.3–5.8 Jy km s^{-1} were reported at Arecibo, while Green Bank fluxes were in the range of 7.4–7.8 Jy km s^{-1}. The discrepancy here is less than our nominal criterion of twice the expected flux ratio, and the mapping reveals no substantial extension of the H I. At the position of UGC 10528 we detect a flux consistent with the high end of the Arecibo measurements. A small amount of H I appears to extend to surrounding positions, giving a total flux consistent with the Green Bank measurements.

13: NGC 7280 (S0). Arecibo fluxes of 1.1–1.6 Jy km s^{-1} were found, while Green Bank fluxes of 2.7–3.8 Jy km s^{-1} were reported. We detect only 1.02 Jy km s^{-1} at the position of this galaxy, but UGCA 429, a dwarf irregular galaxy, is within 3.'8 and is probably confused with the other measurements. The H I from the dwarf irregular appears to extend in the opposite direction of NGC 7280, suggesting that these two galaxies are tidally interacting. The distribution is shown in Fig. 4.

14: NGC 7679 (S0). Arecibo fluxes of 2.5–6.1 Jy km s^{-1} were listed, while fluxes of 9.8–10.5 Jy km s^{-1} were reported at Green Bank and Effelsberg and 14.3 Jy km s^{-1} at the Green Bank 140 foot. Two other galaxies are nearby: NGC 7682 (Sab) at ~4′, which also exhibits discrepant flux measurements, and UGC 12628 (Sc) at ~11′. The higher

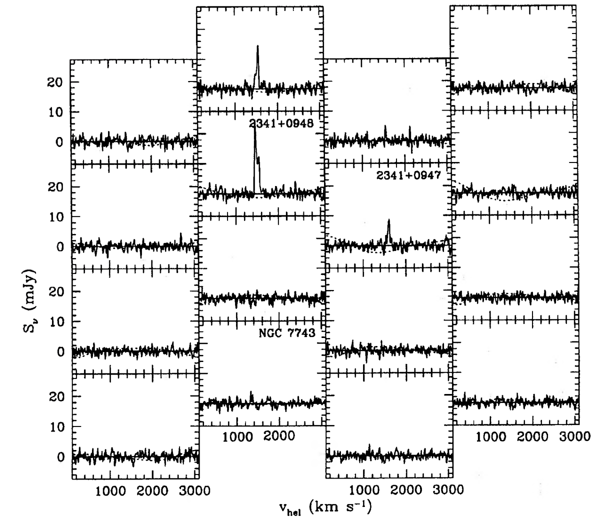

FIG. 5. Portion of H I map around NGC 7743. Points on the hexagonal grid are separated by 3.′8 from their neighbors.

flux measurements for NGC 7679 appear to be confused primarily by NGC 7682. The profile of NGC 7679 is peculiar, and may be somewhat confused even in the Arecibo measurements. The separation from NGC 7682 would normally be sufficient to avoid confusion within the Arecibo beam, however the maps suggest that the H I around NGC 7682 may be slightly extended. The discrepancies appear to be caused mostly by confusion of the two galaxies in the large-beam observations.

15: NGC 7743 (S0). An Arecibo flux of 0.4 Jy km s^{-1} was reported, while Effelsberg and Nançay reported 3.0–3.4 Jy km s^{-1}. We detect nothing at this galaxy's position at an rms level of about 1.5 mJy. The listed detections appear to have been confused by two unusual objects to the north. 2341+0947 is ~8′ north-northwest, it is a narrow-line feature associated with a faint optical counterpart on the Palomar plates. 2341+0948 appears to be a distinct source ~4′ farther northeast, which extends over approximately 3.′2; it is not visible on the Palomar plates even though the H I profile appears to be double horned. The H I distribution is shown in Fig. 5.

TABLE 2. (a). Mapped regions of galaxy groups.

Map # (1)	Name (2)	R.A. Range (3)	Dec. Range (4)	N (5)	Beam Spacing (arcmin) (6)	t_{int} (min) (7)	rms (mJy) (8)
16 ..	Vennik 30	$10^h09.^m3-10^h11.^m0$	03°13′–03°48′	71	3.8	2.0	1.92
17 ..	Vennik 44A	10 45.0 – 10 45.6	27 41 – 29 03	168	7.6	1.5	1.59
18 ..	Vennik 69A+B	12 12.2 – 12 25.5	28 12 – 31 19	179	15.2	1.0	2.18
19 ..	Vennik 91	14 26.2 – 14 28.3	03 09 – 03 44	86	3.8	2.0	2.64
20 ..	Vennik 98A+B	14 58.8 – 15 05.6	01 23 – 02 23	124	7.6	1.5	2.87
21 ..	Vennik 111	22 58.1 – 23 01.2	15 49 – 16 28	126	3.8	1.5	1.39

4. GROUPS OF EARLY-TYPE GALAXIES

We also examined groups of galaxies that, like the M96 group, have a large proportion of early-type galaxies. The groups were selected from the catalog of Vennik (1984), which is substantially similar to the more recent group catalog of Garcia (1993). Vennik cataloged northern galaxy groups out to a redshift of 3200 km s^{-1} using a hierarchical clustering technique, and he also identified possible additional members even when they did not have redshifts.

Vennik's catalog includes 61 groups (or "subgroups" located close to each other) within Arecibo's declination range. About half of the groups contain at least one galaxy classified as Sa or earlier. If we restrict our attention to group members bright enough to have been detected within the entire redshift range of the catalog ($M_B \leqslant -17.5$), only 12 of the groups have at least half of their members of type Sa or earlier. For example, the M96 group (Vennik group 40) has five of these early-type galaxies and only two of later type. In addition, Vennik lists two late-type galaxies that are fainter than the absolute magnitude limit, but the statistics of these dwarf members is much less certain. These groups dominated by early-type galaxies appear to be relatively uncommon, so we wanted to address the possibility that H I in these systems has an unusual distribution like that in the M96 group.

Here we examine six of the groups dominated by early-type galaxies (#30, 44A, 69A, 91, 98A, 98B). In addition, we observed one borderline group (#111) that contained four

TABLE 2. (b) H I measurements in galaxy groups.

Map # (1)	Object (2)	R.A. (3)	Dec. (4)	Type (5)	$\int S\,dv$ (Jy km s^{-1}) (6)	V_{hel} (km s^{-1}) (7)	ΔV_{50} (km s^{-1}) (8)	D (Mpc) (9)	$M_{\rm H\,I}$ ($10^9 M_\odot$) (10)	$\theta_{\rm H\,I}$ (arcmin) (11)	$\theta_{\rm opt}$ (arcmin) (12)	B_T^0 (13)
16	NGC 3156	$10^h10^m05.^s6$	03°22′42″	S0:		— not detected —					1.8	12.91
16	NGC 3165	10 10 58.3	03 37 25	SA(s)dm:	7.9	1356	159	15	0.40	6.4	1.6	13.88
17	NGC 3380	10 45 27.3	28 51 59	SBa p	0.8	1591	104	18	0.063		0.7	14.60
17	UGC 5921	10 46 32.2	28 12 35	Sdm:	3.9	1407	150	18	0.31		1.6	14.20
17	UGC 5958	10 48 31.7	28 04 59	Sbc	1.3	1169	186	18	0.10		1.5	14.27
17	NGC 3414	10 48 31.7	28 12 35	S0p	0.7	1592	256	18	0.055		3.4	11.86
18	UGC 7300	12 14 17.8	29 00 22	Im	8.3	1218	56	13	0.33		1.5	14.71
18	UGC 7302	12 14 17.8	30 31 33	Im:	2.2	3842	71	51	1.4		0.9	~17
18	NGC 4274	12 17 20.2	29 53 33	(R)SB(r)ab		— not detected —					6.9	10.58
19	UGC 9285	14 26 29.5	03 21 42	Scd	1.8	1859	162	22	0.20		1.4	14.04
19	NGC 5636	14 27 07.7	03 29 17	S0+(r)		— not detected —					1.9	13.62
19	NGC 5638	14 27 09.0	03 27 23	E1		— not detected —					2.6	12.06
19	1427+0333	14 27 22.2	03 33 05		1.4	1853	119	22	0.16			
19	UGC 9310	14 27 35.4	03 27 23	SBdm	5.2	1849	144	22	0.59	3.8	2.0	12.86
20	NGC 5838	15 02 54.6	02 17 37	SA0-		— not detected —					3.7	11.71
20	1503+0217	15 03 47.3	02 17 37		1.9	1827	157	24	0.26			
21	UGC 12313–NE	22 59 18.9	15 50 11	Im:	1.7	1971	63	31	0.38		1.5	~16
21	2259+1557	22 59 49.2	15 58 15		3.1	1991	82	31	0.70			
21	NGC 7468	23 00 27.4	16 18 40	E3:p	15.5	2110	108	31	3.5	11.8	0.9	13.80

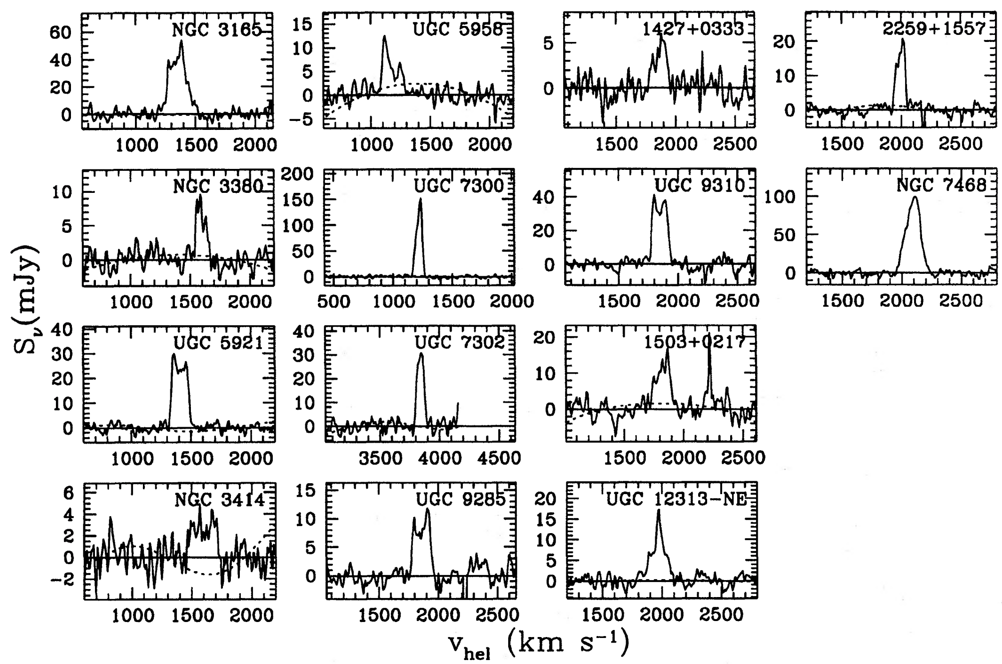

FIG. 6. H I spectra of the objects detected in the maps of early-type galaxy groups, as in Fig. 2.

early-type and five late-type galaxies, and a subgroup (69B) which fell in the same direction as one of the targeted groups. Of the remaining five early-type groups in the Arecibo declination range, Haynes (1981) has partially mapped #31 (NGC 3190 group), and Haynes *et al.* (1979) have mapped #48 (the "Leo triplet") which displays a very extended tidal feature. Individual members of the three other groups (#33, 47, 50) have been previously examined for H I with no obvious peculiarities, but no systematic mapping has been carried out.

General parameters of the mapping procedures are listed in Table 2(a), which follows the same format as Table 1(a), except that the number of the group in Vennik's catalog is given in column (2). Basic results are tabulated in Table 2(b) in the same format as Table 1(b), although we want to stress that in the maps made with coarse grids the H I flux measurements are likely to be quite uncertain. The individual spectra are shown in Fig. 6.

In the descriptions below, after Vennik's group identification, the series of four numbers gives his total count of E/S0/Sa/later-type galaxies within the group with absolute magnitudes $M_B \leqslant -17.5$. We also note the closest corresponding group from Garcia's catalog. For reference, the M96 group has a membership of E/S0/Sa/later galaxies of (2/3/0/2), and Garcia lists it as number 217.

16: Vennik 30 (0/2/1/0). (Garcia 192; NGC 3169 group) The northeast part of this group around NGC 3166 (S0/a) and NGC 3169 (Sa) was mapped by Haynes (1981), who found a complex H I distribution around these galaxies. (NGC 3166 was also identified in the discrepant-flux comparisons, as seen in Fig. 1.) We extend her map to the west and south into the region around the S0 galaxy NGC 3156. We redetect H I in the vicinity of NGC 3165, but no additional sources of H I emission are found.

17: Vennik 44A (0/1/3/1). (Garcia 227; NGC 3414 group) We detect NGC 3414 (S0), NGC 3380 (Sa), UGC 5921 (Sc/Irr), and UGC 5958 (Sb/c). The map points were separated by 7.′6, but we redetected every galaxy that has a previous detection reported in the Huchtmeier & Richter catalog. With this larger spacing our map points were not always close enough to the galaxy center to give an accurate flux or velocity measurement, or an accurate indication of the H I disk size, but we would have detected any very extended features within the group.

18: Vennik 69A (1/2/2/3) & B (1/0/0/3). (Garcia 279; NGC 4274 & NGC 4278 groups) In group 69A, we only clearly detected the Irr galaxy UGC 7300, and we have a probable but uncertain detection of the brightest galaxy, NGC 4274. We also detect a background galaxy UGC 7302. Group 69B has a redshift several hundred km s^{-1} lower, but covers a similar area of the sky and was mapped simultaneously. NGC 4278 also has a wide range of fluxes reported from a number of telescopes. We used a very wide beam spacing of 15.′2 in order to cover these nearby groups' large angular extent. Several galaxies in the region have previously reported detections, but the large beam spacing makes it uncertain that we would detect any but very extended H I regions like the intergalactic ring in the M96 group. (We also note that one row of 14 points was collected at high zenith angle and had a substantially poorer rms noise of 4.8 mJy than the rest of the map.)

19: Vennik 91 (1/2/0/3). (part of Garcia 386; NGC 5638 group) We detect a disk centered on UGC 9310 (Sdm) extending over ~4.′ UGC 9285 (Sc) was also detected. No H I was detected from either NGC 5638 (E) or NGC 5636 (S0/a). We detect a weak H I signal at 1427+0333 that appears to have no visual counterpart on the Palomar plates. There is some chance that this signal could be caused by sidelobe confusion with UGC 9310, but we remapped the immediate vicinity of this source with a 1.′9 spacing, and the signal appears to be confirmed at this position only. On the Palomar plates there are some faint and probably background objects located off-center from the H I signal; without more detailed H I observations we cannot definitively rule them out, but they appear unlikely to be the source of the H I signal. Follow-up optical and H I synthesis observations are clearly needed.

20: Vennik 98A (0/2/0/1) & B (4/2/0/1). (Garcia 392 & 393; NGC 5838 & NGC 5846 groups) This region has two early-type subgroups that are separated by ~400 km s^{-1}, so we were able to search both simultaneously. None of the cataloged galaxies in the region searched has an H I detection, and we did not detect any of them either. However, we did detect a signal at 1503+0217 in the velocity range of group 98B. There is a faint edge-on spiral ~1.′5 west of this position visible on the Palomar plate, which we suspect is the source of the emission. (We also detected a background galaxy UGC 9715 on the edge of one of our 7.′6-spaced beams; this galaxy has been previously detected with much better-suited observations so we do not show it here.)

21: Vennik 111 (3/1/0/5). (Garcia 469; NGC 7448 group) The southern portion of this group was mapped by Haynes (1981) at Arecibo, and by van Driel *et al.* (1992) at Westerbork. Our map extends north from the north end of Haynes' map. There is a complex H I distribution around the southern group members including NGC 7464 (E pec) and NGC 7465 (S0), with possible tidal tails of H I. NGC 7448 (Sbc) also shows unusual noncorotating gas in its outer parts. We extended the map over the rest of the group and detect a large disk centered on NGC 7468 (E pec), a Markarian galaxy (Mkn 314). The disk extends over ~11′ as shown in Fig. 7. Taylor *et al.* (1993) also observed this galaxy at the VLA as part of a study of "H II galaxies" and detect H I over an 8′ extent separated into two separate features, one of which they associate with an edge-on spiral north of NGC 7468. We detect about 50% more H I than they do, and our spectra do not appear consistent with rotation of an edge-on galaxy, so we suspect that they may have "resolved out" some of the more widespread emission that would suggest this is actually an extended disk. In addition, we detect the northeast portion of UGC 12313 at the edge of our map as well as a signal at 2259+1557. This latter signal was found close to position "N5" observed at Nançy by van Driel *et al.* (1992), and it shares the same velocity. However, we do not believe it is associated with a diffuse cloud since there is a small, low surface brightness object on the Palomar plates near the position where the flux peaks.

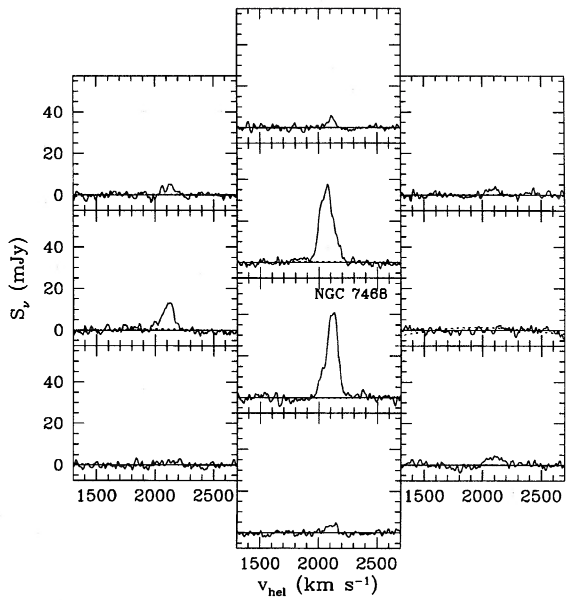

FIG. 7. H I map around NGC 7468. Points on the hexagonal grid are separated by 3.′8 from their neighbors.

5. DISCUSSION

The number of early-type galaxies with unusual, extended H I distributions is surprisingly large. As a class, the early-type galaxies are the most likely to show discrepant fluxes in previous observations, and our observations indicate that most of the discrepancies were genuine. Of the 14 early-type galaxies (Sa and earlier) with a discrepancy of a factor of 2 or more, only five appeared to be caused by inaccurate measurements. Three appear to have extended disks significantly larger than their optical dimensions, and seven (including one of the extended-disk galaxies) were caused by confusion. The category of confused objects is more interesting than its name would suggest since most of them are caused by faint galaxies or photographically unidentified sources in close proximity to the early-type galaxies. In addition, the early-type groups (including several that were studied previously) appear to have a high incidence of unusual H I features, although this is less easily quantified.

Large hydrogen extents have been detected in a variety of galaxy types, although the frequency of the phenomenon is not well established. In late-type dwarf irregular galaxies, a number of systems have been found with extremely extended H I. One of the more interesting cases studied by Hoffman *et al.* (1993) is DDO 137 and its companion NGC 4532, which exhibit a large horseshoe-shaped cloud. The "protogalaxy" found by Giovanelli & Haynes (1989) in the Virgo cluster is an extreme example of a very large hydrogen feature surrounding a very small optical region. Surveys of spiral galaxies show occasionally large H I disks (e.g., Briggs *et al.* 1980), and it sometimes seems that almost every gas-rich galaxy that is studied in depth shows H I extending well beyond the optical disk, up to many times the Holmberg radius, as in Markarian 348 (Morris & Wannier 1980; Simkin *et al.* 1987).

We can use the two-telescope flux comparisons from Sec. 3 to estimate the relative frequency of extended H I in different types. Over half of the E-S0/a galaxies with useful observations at both Arecibo and Green Bank (or Efflesburg) showed discrepancies suggesting extended H I. Only 12% of the Sa-Sab, and <1% of the Sb-Sd galaxies showed similar discrepancies. Some caution should be exercised in interpreting these statistics, since early type galaxies have a relatively small amount of H I within their disks, so it is possible that external H I might be easier to detect by contrast. However, the mean H I mass of the early-type galaxies examined here was only two to three times lower than for the classes of spiral galaxies. Moreover, the galaxies with discrepant fluxes have H I masses well within the range of masses exhibited by the late-type galaxies, so the lack of discrepant fluxes among these low-H I mass, late-type galaxies represents a real difference.

Among the early-type groups identified from Vennik's catalog, roughly half display unusual H I structures, and the fraction of individual early-type galaxies with unusual H I features appears similar to the fraction for the overall population of early-type galaxies. It is difficult to calibrate these statistics since there are no comparable studies of the later-type groups. Furthermore, the groups with the most spectacular H I features are actually drawn from earlier studies, leading to some worry that *a posteriori* statistics may be inflating the percentage of exceptional early-type groups. It is also of note that in clusters—where ellipticals and lenticulars dominate the population—H I is less evident. However, this may be because the neutral gas cannot survive in the hot intracluster medium (and it may even be a source for the intracluster gas). In any case, it appears that membership in low density groups allows extended H I features to form, but group membership is not necessary given that several of the galaxies with extended H I features, including the most extreme example of NGC 5701, are in quite isolated regions.

The unusual distributions of H I associated with early-type galaxies may provide evidence of the gas's origin. Huchtmeier *et al.* (1995) found that H I-rich ellipticals tend to be more common in compact groups, suggesting that interaction with nearby companions may be a source of the gas. Some ellipticals show evidence that the gas may derive from disrupted dwarf companions (Patterson & Thuan 1992; Schweizer *et al.* 1989) or generated through mergers between former disk galaxies (Schiminovich *et al.* 1995).

Sorted into the appropriate order, our observations appear to support and extend the accretion scenario. We observe distinct dwarf neighbors, dwarf neighbors that appear tidally distorted or otherwise peculiar, and extended, sometimes irregular disks surrounding the early-type targets of our survey. The ring and extended disk distributions found by van Driel & van Woerden (1991) also indicate gas with a high angular momentum, perhaps reflecting the original orbital angular momentum of a former companion. In this circumstance, the gas might remain outside the disk for a long period in a diffuse state with little star formation.

To explain the frequency of this phenomenon around early-type galaxies relative to later-type galaxies, we can suggest three possibilities. In general, the early-type galaxies tend to be more massive and perhaps therefore more effective at tidally disrupting dwarf companions. In addition, comparably massive spirals also tend to have larger amounts of H I within their disks and they might therefore mask the presence of external gas. Finally, the larger amounts of gas in later-type galaxies would probably shorten the lifetime of these extended features through direct hydrodynamical interactions.

In conclusion, the observations of early-type galaxies show H I in a range of stages suggesting the accretion of H I-rich neighbors. We suspect the process is particularly evident in gas-poor galaxies in large part because there is less difficulty in detecting the incremental addition of gas. Taken together with observations like those of Taylor *et al.* (1993) of H I companions to late-type galaxies, this suggests that accretion of gas-rich companion galaxies is a continuing process among all galaxies to the present epoch.

We would like to thank the telescope operators and staff of the Arecibo observatory for their friendly assistance throughout these observations. This work was supported in part by NSF Presidential Young Investigator award AST-9158096.

REFERENCES

Binggeli, B., Sandage, A., & Tammann, G. A. 1985, AJ, 90, 1681

Briggs, F. H., Wolfe, A. M., Krumm, N., & Salpeter, E. E. 1980, ApJ, 238, 510

Corbelli, E., Schneider, S. E., & Salpeter, E. E. 1989, AJ, 97, 390

de Vaucouleurs, G., de Vaucouleurs, A., Corwin, H. G., Buta, R. J., Paturel, G., & Fouque, P. 1991 Third Reference Catalogue of Bright Galaxies (Springer, New York)

Eder, J. Giovanelli, R., & Haynes, M. P. 1991, AJ, 102, 572

Garcia, A. M. 1993, A&AS, 100, 47

Giovanelli, R., & Haynes, M. P. 1989, ApJ, 346, L5

Haynes, M. P. 1981, AJ, 86, 1126

Haynes, M. P., Giovanelli, R., & Roberts, M. S. 1979, ApJ, 229, 83

Helou, G., Hoffman, G. L., & Salpeter, E. E. 1984, ApJS, 55, 433

Hickson, P., de Oliveira, C. M., Huchra, J. P., & Palumbo, G. G. C. 1992, ApJ, 399, 353

Hoffman, G. L., Lewis, B. M., Helou, G., Salpeter, E. E., Williams, H. L. 1989, ApJS, 69, 65

Hoffman, G. L., Lu, N. Y., Salpeter, E. E., Farhat, B., Lamphier, C., & Roos, T. 1993, AJ, 106, 39

Huchtmeier, W. K., & Richter, O. G. 1989, A General Catalog of H I Observations of Galaxies (Springer, Berlin)

Huchtmeier, W. K., Sage, L. J., & Henkel, C. 1995, A&A, 300, 675

Lo, K.-Y., & Sargent, W. L. W. 1979, ApJ, 227, 756

Morris, M., & Wannier, P. G. 1980, ApJ, 238, L7

Oosterloo, T. 1988, thesis, University of Groningen

Patterson, R. J., & Thuan, T. X. 1992, ApJ, 400, L55

Schiminovich, D., Van Gorkom, J. H., Van der Hulst, J. M., & Malin, D. F. 1995, ApJ, 444, L77

Schneider, S. E. 1989, ApJ, 343, 94

Schneider, S. E., Helou, G., Salpeter, E. E., & Terzian, Y. 1986, AJ, 92, 742

Schweizer, F., Van Gorkom, J. H., & Seitzer, P. 1989, ApJ, 338, 770

Simkin, S. M., Su, M., Van Gorkom, J., & Hibbard, J. 1987, Science, 235, 1367

Takase, B., & Miyauchi-Isobe, N. 1986, Ann. Tokyo Astron. Obs., Ser. 2, 21, 127

Taylor, C. L., Brinks, E., & Skillman. E. D. 1993, AJ, 105, 128

van Driel, W., *et al.* 1992, A&A, 259, 71

van Driel, W., & van Woerden, H. 1991, A&A, 243, 71

Vennik, J. 1984, Tartu Astrofuus. Obs. Teated, 73, 1